Aquatic Toxicology 194 (2018) 57–66

Contents lists available at ScienceDirect

Aquatic Toxicology

journal homepage: www.elsevier.com/locate/aqtox

Gadolinium perturbs expression of skeletogenic genes, calcium uptake and larval development in phylogenetically distant sea urchin species

Chiara Martino[a,b,*,1], Caterina Costa[b,1], Maria Carmela Roccheri[a], Demian Koop[c], Rosaria Scudiero[d], Maria Byrne[c]

[a] Dipartimento Scienze e Tecnologie Biologiche Chimiche e Farmaceutiche, Università di Palermo, Viale delle Scienze, Ed. 16, 90128, Palermo, Italy
[b] Consiglio Nazionale delle Ricerche, Istituto di Biomedicina e Immunologia Molecolare "Alberto Monroy", Via Ugo La Malfa 153, 90146, Palermo, Italy
[c] Department of Anatomy and Histology, F13, University of Sydney, NSW, Australia
[d] Dipartimento di Biologia, Università di Napoli Federico II, via Mezzocannone 8, 80134, Napoli, Italy

ARTICLE INFO

Keywords:
Sea urchin embryos
Medical agent
Skeletogenesis
Marine pollution
Gene expression
Ecotoxicology

ABSTRACT

Chelates of Gadolinium (Gd), a lanthanide metal, are employed as contrast agents for magnetic resonance imaging and are released into the aquatic environment where they are an emerging contaminant. We studied the effects of environmentally relevant Gd concentrations on the development of two phylogenetically and geographically distant sea urchin species: the Mediterranean *Paracentrotus lividus* and the Australian *Heliocidaris tuberculata*. We found a general delay of embryo development at 24 h post-fertilization, and a strong inhibition of skeleton growth at 48 h. Total Gd and Ca content in the larvae showed a time- and concentration-dependent increase in Gd, in parallel with a reduction in Ca. To investigate the impact of Gd on the expression of genes involved in the regulation of skeletogenesis, we performed comparative RT-PCR analysis and found a mis-regulation of several genes involved in the skeletogenic and left-right axis specification gene regulatory networks. Species-specific differences in the biomineralization response were evident, likely due to differences in the skeletal framework of the larvae and the amount of biomineral produced. Our results highlight the hazard of Gd for marine organisms.

1. Introduction

Pharmaceuticals and agents used for medical applications are commonly detected in the aquatic environment and are increasingly of global concern (Brausch et al., 2012; Brooks and Huggett, 2012; Tiwari et al., 2017), but their impact on aquatic and marine organisms is still poorly understood (Boxall et al., 2012). These agents are manufactured to be biologically active compounds with specific cellular targets that, if evolutionarily conserved, are likely to affect a broad spectrum of species and so present a high ecotoxicological risk (Gunnarsson et al., 2008). Compounds released into the environment that interact with evolutionarily conserved transporter or receptor proteins are of particular concern for marine biota (Berninger and Brooks, 2010; Fong and Ford, 2014).

Gadolinium (Gd), despite being one of the rarest elements on Earth (Lide et al., 2009), is a medical agent recognized as an emerging environmental pollutant (Telgmann et al., 2013). Chelates of this element have been used as contrast agents in magnetic resonance imaging (MRI) since the 1980s. Although originally considered to be safe for humans (Niendorf et al., 1991; Joffe et al., 1998), Gd chelates have been shown to be dangerous for human health and linked to the development of a cutaneous disease, the nephrogenic systemic fibrosis (Cowper et al., 2000; Grobner, 2006). Gd-based MRI contrast agents are generally very stable complexes. After being rapidly eliminated from the patient's body, they are released into waste-water systems and are not removed in the treatment of effluents (Telgmann et al., 2013). Thus, Gd chelates are released largely unchanged into aquatic and marine environments (Telgmann et al., 2013), where their occurrence has significantly increased over the last 20 years (Zhu et al., 2004; Hatje et al., 2016).

Gd toxicity on aquatic organisms is poorly understood. In freshwater mussels Gd exposure triggers mitochondrial and anti-inflammatory pathways (Hanana et al., 2017), and in goldfish Gd accumulates in the liver and induces antioxidant enzyme production (Chen et al., 2000; Laville et al., 2004). The high toxicity of Gd ions (Gd^{3+})

Abbreviations: hpf, hours post fertilization; Gd, gadolinium; GAT, gadolinium acetate tetrahydrate; Ca, calcium; PMCs, primary mesenchyme cells; WF, washed free; GRN, gene regulatory network

* Corresponding author at: Dipartimento Scienze e Tecnologie Biologiche Chimiche e Farmaceutiche, Università di Palermo, Viale delle Scienze, Ed. 16, 90128, Palermo, Italy.
E-mail address: chiara.martino@unipa.it (C. Martino).

[1] These authors equally contributed to the work.

https://doi.org/10.1016/j.aquatox.2017.11.004
Received 23 June 2017; Received in revised form 6 November 2017; Accepted 9 November 2017
Available online 11 November 2017
0166-445X/

appears to be associated with its action as a blocker of calcium channels, as its ionic radius (0,938 Å; 93,8 pm) is nearly equal to that of divalent Ca^{2+} (0,99 Å; 99 pm) (Sherry et al., 2009). Gd^{3+} is able to compete with Ca^{2+} in physiological processes requiring Ca^{2+}, usually binding with much higher affinity than Ca^{2+} (Mlinar and Enyeart, 1993; Sherry et al., 2009).

Sea urchin embryos and larvae living in the water column face many adverse environmental conditions and pollutants (Lawrence, 2013). These marine invertebrates have been used as a model system for decades to evaluate the potential risk of pollutants in the marine environment (Byrne et al., 2013; Matranga et al., 2013; Bonaventura and Matranga, 2017; Chiarelli et al., 2016). Sea urchin larvae have a calcite ($CaCO_3$) endoskeleton containing 5% of magnesium carbonate and 0.1% of occluded matrix proteins (Matranga et al., 2011). Skeletogenesis is initiated at the gastrula stage by the primary mesenchyme cells (PMCs), descendants of the micromeres (Wilt, 2005). Gene expression in these cells is required for specification of the skeletogenic lineage and biomineral formation (Oliveri et al., 2008). At the gastrula stage, PMCs are interconnected in a syncytium and arranged in the blastocoelic cavity in a characteristic spatial pattern forming a sub equatorial ring linking two ventrolateral clusters (Matranga et al., 2011). Spiculogenesis starts with the deposition of a calcite crystal within the syncytium in each cluster (Wilt, 2005). These skeletal rudiments extend in triradiate spicules, which then grow along three spatial directions to form the larval skeleton (Wilt, 2005). Calcium contained in the spicules is obtained from seawater, where it occurs at high concentration (~10 mM) (Vidavsky et al., 2016). PMCs possess active Ca^{2+} transporters, presumably with high capacity and low affinity, but they have not yet been identified (Vidavsky et al., 2016). The larval skeleton is highly sensitive to environmental stressors and so is a trait often used for ecotoxicology (Matranga et al., 2011). Proper skeletogenesis depends on the dynamic interactions of genes in a complex Gene Regulatory Network (GRN) (Oliveri et al., 2008). PMCs express a unique suite of genes that function in skeletogenesis. The molecular cross-talk between the PMCs and the ectoderm is essential to achieve the complex three-dimensional structure of the skeleton and its bilateral symmetry, as well as the spatial organization of PMCs (Duloquin et al., 2007; Röttinger et al., 2008).

Several studies have examined the impact of toxicants, including metals (e.g. Cd, Mn, Pb, Zn) and other stressors (e.g. UV, X-rays, sulfamethoxazole) on gene expression during sea urchin development, with a focus on the skeleton as a sensitive trait for ecotoxicology (Russo et al., 2003, 2010; Bonaventura et al., 2005; Matranga et al., 2010; Pinsino et al., 2011; Ragusa et al., 2013). Overall, these studies document altered gene expression, including genes involved in skeletogenesis (e.g. *sm30, sm50, msp130*) (Bonaventura et al., 2005; Matranga et al., 2010; Pinsino et al., 2011) and in stress, apoptotic and inflammatory responses (e.g. *hsps, metallothionein, 14-3-3, fadd, casp8, bak, pin, ptprd, tak)* (Bonaventura et al., 2005; Russo et al., 2003, 2010; Ragusa et al., 2017). Thus far, however, the impact of environmental xenobiotics on expression of the genes involved in the skeletogenic GRN has not been fully examined. With respect to the impact of toxicants on Ca content of sea urchin larvae as an indicator of impaired calcification, Pinsino et al. (2011) found that the endogenous Ca^{2+} levels were strongly reduced by manganese exposure, as measured by atomic absorption spectrometry. Tellis et al. (2014) suggest that toxic metals may interfere with Ca homeostasis in sea urchin development.

In a previous study, a wide range of sublethal Gd concentrations (1 nM–200 μM) was tested on embryos and larvae (from fertilization to the pluteus stage) of four phylogenetically and geographically distant species, two living in the Mediterranean Sea, *Paracentrotus lividus* and *Arbacia lixula,* and two living in the Australian East Coast, *Heliocidaris tuberculata* and *Centrostephanus rodgersii* (Martino et al., 2017a). A strong concentration-dependent response to Gd was found in all species, mainly affecting skeleton formation, with species-specific threshold levels of sensitivity (Martino et al., 2017a). The different sensitivities emphasized the importance of testing toxicity in a range of species when assessing the impacts of xenobiotics entering the marine environment (Martino et al., 2017a). The morphological aberrations caused by Gd were categorized in different larval morphotypes, highlighting the severe inhibition of growth and patterning of the larval skeleton (48 h post fertilization, hpf) of the four species, including left-right asymmetry in skeleton development (Martino et al., 2017a). In a subsequent study of *P. lividus* embryos exposed to Gd 20 μM, Martino et al. (2017b) showed that the PMCs were correctly localized at 24 hpf, but not at 48 hpf, and that the stress response was associated with a significant induction of autophagy, a known cell survival mechanism in sea urchin embryos (Agnello et al., 2016; Chiarelli et al., 2016; Martino et al., 2017b).

We extended on our research focusing on two species, *P. lividus* and *H. tuberculata*, to investigate the link between skeletogenesis, calcium homeostasis and expression of skeletogenic genes in embryos treated with Gd. The two species were chosen based on their similar morphological response but different sensitivity to this agent and their contrasting skeletal robustness (Martino et al., 2017a). The latter is important as development of skeleton is a response variable often used for ecotoxicology and is a trait that can vary greatly in sensitivity between species, likely due to evolutionary/phylogenetic differences (Zito et al., 2015; Martino et al., 2017a).

Here, for the first time, we investigated the expression of 12 genes in response to the emerging toxicant Gd. We focused on genes involved in the regulation of skeletogenesis from three functional levels as indicated by the skeletogenic GRN (Oliveri et al., 2008): i) early expressed genes, including genes involved in the left/right specification axis (*nodal, lefty, bmp*) and *alx-1*, a primary driver of skeletogenic specification and differentiation; ii) signaling molecule genes involved in the ectoderm-PMCs induction that regulates skeletogenesis and which are essential for directional migration of the PMCs (*univin, vegf, vegf-r, fgf*); iii) skeletogenic genes needed for the deposition of the biomineral (*msp130, sm30, p16, p19*). As Gd is a known blocker of calcium channels, we also investigated the relationship between Gd exposure, skeletal growth and calcium uptake by Flame Atomic Absorption Spectrometry (FAAS). This allowed us to assess the impact of Gd on calcium uptake during development and the potential perturbation of genetic control of the biomineralization process.

2. Materials and methods

2.1. Embryo cultures, exposure to Gd and morphological analysis

Paracentrotus lividus were collected along the North-Western coast of Sicily, Italy. *Heliocidaris tuberculata* were collected from Little Bay, Sydney, Australia (under permit from NSW DPI). Eggs were fertilized and embryos were cultured as previously described (Martino et al., 2017a). Embryos were reared at 18–20 °C in Millipore filtered seawater (MFSW). Just after fertilization, the embryos were exposed to Gadolinium Acetate Tetrahydrate (GAT, Waco) at different concentrations: 20 μM for *P. lividus;* 500 nM and 5 μM for *H. tuberculata* (*Pl*-EC50: 1.18 μM; *Ht*-EC50: 56 nM). These concentrations were chosen based on the Gd concentration-response curve determined for these species (Martino et al., 2017a). For *P. lividus,* 20 μM was the concentration with highest percentage of larvae that had an asymmetrical skeleton. For *H. tuberculata,* 500 nM was the concentration that caused the highest percentage of asymmetrical embryos, and 5 μM was the concentration with the highest percentage of embryos without any skeleton (Martino et al., 2017a). The GAT salt was freeze-dried before weighing and then dissolved in MFSW. Three recovery experiments were performed as previously described in *P. lividus* embryos (Martino et al., 2017b). Briefly, Gd was removed after 24 h of development/exposure by washing embryos three times in MFSW by hand centrifugation, and then these washed free (WF) embryos were cultured in MFSW for further 24 h. Embryos were microscopically inspected (Zeiss Axioscop 2

plus or Olympus BX60) at different endpoints and photographed using a digital camera. At 6, 24 and 48 hpf, the embryos were collected and centrifuged at low-speed at 4 °C. The supernatant seawater was removed and the embryos were flash frozen in liquid nitrogen and stored at −80 °C until use.

2.2. Determination of gadolinium and calcium content in the larvae

As skeletal spicules are calcareous structures, Ca is needed to construct the skeleton. To investigate the relationship between Gd exposure, skeleton growth and calcium uptake, the total amount of Ca and Gd in the larvae of the two species was analysed by Flame Atomic Absorption Spectrometry (FAAS) in three independent experiments. Frozen embryos were prepared for metal determination by acid digestion in 70% HNO_3/30% H_2O_2 (v/v 2:1) at 150 °C in oil bath. The dried residues were reconstituted in 0.2% HNO_3 and analysed for metal contents by FAAS using a Perkin Elmer Analyst 800 apparatus. The total Ca and Gd content data were determined for the embryos from each fertilization with means presented (n = 3, ± Standard Deviation − SD).

2.3. RNA extraction

Total RNA from control and Gd-exposed embryos (6, 24 hpf) and larvae (48 hpf) was extracted from frozen pellets of nine biologically independent replicates of *P. lividus and H. tuberculata* embryos. The embryos from each fertilization were generated from the gametes of multiple parents and were placed in 9 separate wells in culture dishes (3 from each fertilization). As each of the wells would contain a different set of embryo genotypes, they were regarded as independent replicates, thus n = 9. The RNA extraction was performed using the GenElute Mammalian Total RNA Miniprep Kit™ (Sigma), and the RNeasy Mini Kit (Qiagen) respectively for *P. lividus* and *H. tuberculata* embryos. Residual DNA was eliminated by DNase I (Sigma) digestion. The RNA purity and quantity were estimated using a bio-photometer (Eppendorf) or a NanoDrop Spectrophotometer (Thermo Scientific). All samples were diluted to the same concentration and frozen at −20 °C until use.

2.4. Gene selection, oligo design and One Step RT-PCR

In a preliminary analysis of the sea urchin skeletogenic GRN, 12 target genes were selected and their sequences were retrieved from the NCBI nucleotide database. In order to perform expression analysis by amplification reactions, specific couples of forward and reverse primers were drawn and evaluated by Blast search at NCBI (Table 1). MWG (Heidelberg, Germany) and IDT (Singapore) services were utilized for primer synthesis. *Pl-nodal* and *Pl-fgf* primers were kindly provided by Dr. Cavalieri (University of Palermo) (Cavalieri and Spinelli, 2014; Cavalieri et al., 2011).

Superscript One-Step RT-PCR kit (Invitrogen) was utilized to perform comparative gene expression assays and detect differences between controls and treated embryos as in previous studies (Russo et al., 2003; Matranga et al., 2010; Costa et al., 2010; Antiabong et al., 2016). Equal amount of total RNA from control and Gd-exposed embryos were used to amplify the selected RNA targets and reference genes (Costa et al., 2012). S24 and Z12 genes, encoding respectively a ribosomal protein and a zinc-finger transcription factor, were used as internal reference genes for *P. lividus* and *H. tuberculata* embryos, respectively, as they were found to have constant level of expression throughout development (Sgroi et al., 1996; Costa et al., 2012).

The One Step RT-PCR reactions were performed according to the manufacturer's instructions. The RT was always carried at 50 °C for 30 min, followed by a denaturation step of 2 min at 94 °C. Depending on the primer set with specific annealing temperature, the amplification step had a variable number of amplification cycles (26–35) in order to keep a logarithmic trend in every reaction. After amplification, a final extension step for 10 min at 72 °C was performed. The RT-PCR reactions were analysed by electrophoresis on agarose gel. After running, gel acquisitions were carried out using GelDoc1000 imaging detection system (BioRad) and the FluorChem E digital imaging system (Alpha Innotech). Densitometric analysis of gel bands was performed using the Quantity One image analysis software, version 1.1 (BioRad). The comparison of relative expression levels of the genes between control and Gd-exposed embryos was obtained by normalizing amplicon band intensities to the values of the genes used as internal reference.

2.5. Statistical analysis

The One Step RT-PCR data are presented as the mean of the 9 independent reactions ± SD (from embryos harvested from 9 wells) for each developmental endpoint (6, 24 and 48 hpf) for each gene. These data were analysed by the one-way analysis of variance (ANOVA). Homogeneity of variance was checked using the Levene's test. Tukey's HSD test was used as post-hoc test analysis of significant differences. The analyses were performed using the Statistica 13.2 software (StatSoft, Tulsa, OK, USA), and the level of significance was set to $P < 0.05$.

Table 1
List of primer sequences used for gene expression analysis, number of cycles and annealing temperature (°C).

Name	Forward primer 5′-3′	Reverse primer 5′-3′	Number of Cycles	Annealing T (°C)
Pl-Alx1	GCCGTGTCTAGCTACATACC	GTACACATCGGGTAGTG C	30	55
Pl-fgf	TACATTTGAAGTGGTTGGATTTCG	GCCAGGGACACGCATAAGAAC	30	55
Pl-msp130r1	CAAGGGAAATCCAAGATGGCGTTG	TCTCTCTGGCTGGACCCTCAT	30	55
Pl-nodal	ACAACCCAAGCAACCACGCA	CGCACTCCTGTACGATCATG	30	55
Pl-p16	ATGAAGACTTTTGTTGCCCTCTTGTC	CGCGTTTTGAAGCATCTGGGC	30	55
Pl-p19	ATGACCAAGGAAGAGGCTGC	GTGGTCCCATTACCATTTCACTG	30	55
Pl-S24	CTGATCAGACCATGCTCTAAGGT	CCTGATGTCGTCAGTACAACGTA	30	55
Pl-univin	GTCTGCAACTGTTGGACGTC	GAAAGGGCATTCACCATCGC	34	55
Pl-vegf	GACTGTCCGAACAACAAGGTC	GATTCCAGTCTCTGGGACAAG	30	55
Pl-vegfr	GTCGACGACTCATACATCATCC	TAA GGC GTA CCG GTG ATC AC	30	55
Ht-bmp2-4	GGCCGAATTGAGATTGTTTCG	TTTGAGCGTCTTGAGGATGG	26	54
Ht-fgf	TCGCACGTAATCATCATCGG	TCAGGCATCTTGTAAGCATAGG	35	54
Ht-lefty	GTCGTCAACCAACACAATGG	AAGTTAGCAGTGGAGGAATGG	26	54
Ht-msp130	TCCTATGATTCCCACCACGC	AAGGTCATGTTCCGGGTCAC	26	54
Ht-nodal	TAACCATGCATCGACCATCC	GGTAGACTCCTCACTTGAAACG	30	54
Ht-sm30B	AAACTACACCAACTGGGAAGG	CTGAGGAATGGCTGAGATAACG	21	54
Ht-vegf2	ATGATTACGGAGATGGGTATGG	GGCATTATGATAGTGGTAGTTTCG	35	54
Ht-Z12	AGTGCTGTTCAAGATGCGGA	CTCTCCTGTATGGACACGCC	26 − 35	54

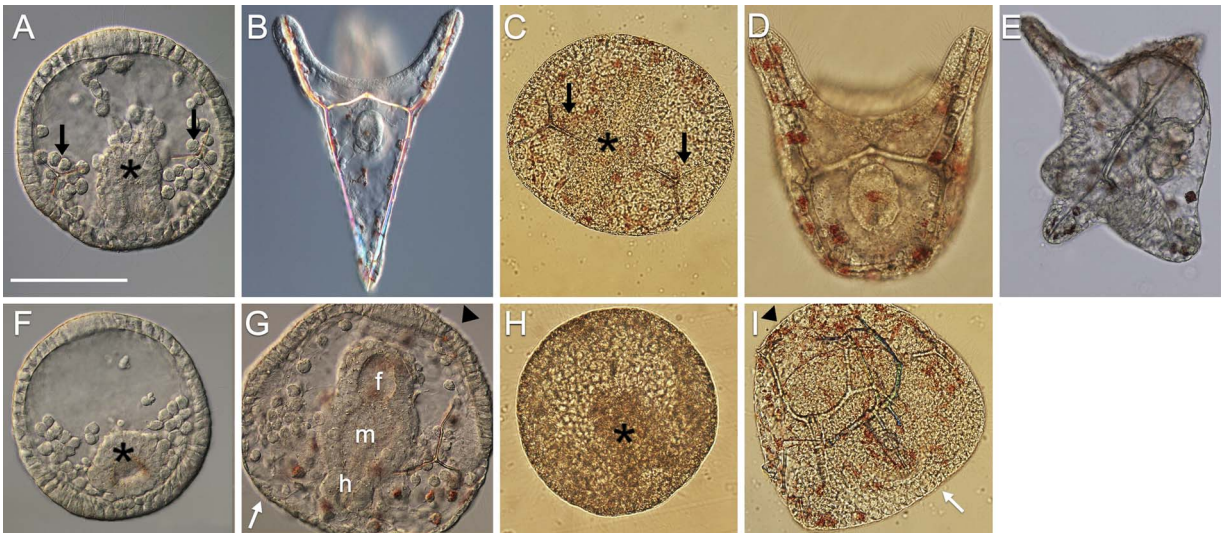

Fig. 1. Representative pictures of controls (A–D), Gd-exposed (F–I), and WF (E) embryos and larvae of the two species after 24 (A, C, F, H) and 48 (B, D, E, G, I) hpf. (A, B, E, F, G) *P. lividus* embryos; (C, D, H, I) *H. tuberculata* embryos. Black arrows, triradiate spicules; asterisks, gut formation; white arrows, squamous epithelium cells; arrowheads, columnar oral epithelium. h, hindgut; m, midgut; f, foregut. Bar = 50 μm in A, C, F, G, H I; 25 μm in B, D, E.

3. Results

3.1. Gd exposure perturbs embryo development

Paracentrotus lividus and *H. tuberculata* exhibited a similar morphological response to Gd (Fig. 1). In both species, the PMC ingression appeared to be normal (Fig. 1A, F) and archenteron invagination occurred on schedule (Fig. 1A, C, F, H, see asterisks). The first effects of Gd were visible at the gastrula stage (24 hpf), at the onset of skeletogenesis. The two triradiate spicules were present in controls (Fig. 1A and C, see black arrows), but the Gd-exposed embryos lacked spicules (Fig. 1F, H). At 48 hpf, the controls were echinoplutei with a well-developed larval skeleton (Fig. 1B, D). The plutei of *P. lividus* (Fig. 1B) have an elongated body, with unfenestrated thin skeletal rods, while *H. tuberculata* plutei have wider body with robust and fenestrated arm rods (Fig. 1D). At 48 hpf, in both controls and Gd-exposed embryos, the ectoderm was patterned along the oral-aboral axis (Fig. 1G, I), with the squamous aboral epithelium at the vegetal pole (Fig. 1G, I, see white arrows) and the columnar oral epithelium at the animal pole (Fig. 1G, I, see arrowhead). In control and treated embryos, the archenteron was correctly differentiated into a tripartite gut (Fig. 1G, see f, m, h) and differentiation of circumesophageal muscle cells was complete. The characteristic contractile movements of the gut were also observed.

It appears that Gd-exposure mainly affected skeleton formation in both species, resulting in a range of abnormalities with a severe inhibition of skeleton growth and patterning in treated embryos (Fig. 1G, I). In both species, some embryos showed a severe disorganization of the skeletal rods with formation of supernumerary rods resulting in the inability to achieve the pluteus form (Fig. 1I). Some embryos had shorter spicules leading to a reduction of arm length, while others had an asymmetric skeletal pattern (Fig. 1G). In *P. lividus,* WF embryos showed a partial recovery of skeleton elongation. However, the skeleton pattern was abnormal (Fig. 1E).

3.2. Gadolinium-induced inhibition of spicules growth correlates with calcium uptake during development

To investigate the relationship between Gd exposure, Ca uptake and skeleton growth we analysed the Ca and Gd content by FAAS in controls, Gd-exposed embryos and WF embryos.

The histogram in Fig. 2A shows the amount of Ca in *P. lividus* embryos. Control larvae at 48 hpf had a 10-fold higher total amount of Ca than at 24 hpf (40.49 μg/mg ± 3 SD *vs* 4.04 μg/mg ± 0.4 SD), reflecting the skeleton production resulting in the formation of a complex three-dimensional skeleton (Fig. 1A, C). In Gd-treated embryos there was a 45.54% reduction in the amount of Ca compared to controls at 24 hpf (4.04 μg/mg ± 0.4 SD in controls *vs* 2.2 μg/mg ± 0.2 SD in Gd-exposed embryos), and a 78.81% reduction at 48 hpf (40.49 μg/mg ± 3 SD in controls *vs* 8.58 μg/mg ± 1.2 SD in Gd-exposed embryos). The increase in Ca levels during development in Gd-exposed embryos was weak if compared to controls, as the total amount of Ca was only 4.72-fold higher at 48 hpf than at 24 hpf. WF embryos had an intermediate value of Ca amount (19.2 μg/mg ± 0.9 SD) between 48 hpf-controls and embryos continuously exposed to Gd for 48 h, with a 52.58% reduction with respect to controls (Fig. 2A).

Fig. 2B shows the amount of Gd in controls and treated embryos. No Gd was detectable in controls (< 5 ng, the resolution limit of the instrument), while Gd-exposed embryos had 427.8 ng/mg ± 60 SD at 24 hpf and 674.66 ng/mg ± 49 SD at 48 hpf. Strikingly, WF embryos had an amount of Gd (276.26 ng/mg ± 37 SD) intermediate between the 48 hpf-controls and embryos that were continuously exposed to Gd for 48 h.

As for *P. lividus*, the total amount of Ca increased during development in *H. tuberculata* control embryos, being 13.8-fold higher at 48 hpf (69.69 μg/mg ± 3.48 SD) than at 24 hpf (5.05 μg/mg ± 0.25 SD). In Gd-exposed *H. tuberculata* embryos we found an 80% reduction in the amount of Ca at both concentrations at 24 hpf (5.05 μg/mg ± 0.25 SD in controls *vs* 1.01 μg/mg ± 0.26 SD in Gd-exposed embryos) and a 90% reduction at 48 hpf at both concentrations (69.69 μg/mg ± 3.48 SD in controls *vs* 6.91 μg/mg ± 0.34 SD in 500 nM Gd and 6.66 μg/mg ± 0.48 SD in 5 μM Gd) (Fig. 3A). Thus, the lowest Gd concentration tested (500 nM) was sufficient to block calcium uptake. No Gd was detectable in controls (< 5 ng), while a concentration-response effect was observed in Gd-exposed embryos, with a greater Gd amount at the highest concentration tested both at 24 hpf (7.4 ng/mg ± 0.07 SD at 500 nM *vs* 320.64 ng/mg ± 16.03 SD at 5 μM) and at 48 hpf (380.16 ng/mg ± 19 SD at 500 nM *vs* 1040.51 ng/mg ± 52.71 SD at 5 μM) (Fig. 3B).

3.3. Gd exposure perturbs expression of skeletogenic genes

To determine the temporal expression of several transcripts involved in the regulation of skeletogenesis, we carried out analysis of mRNA expression of candidate genes.

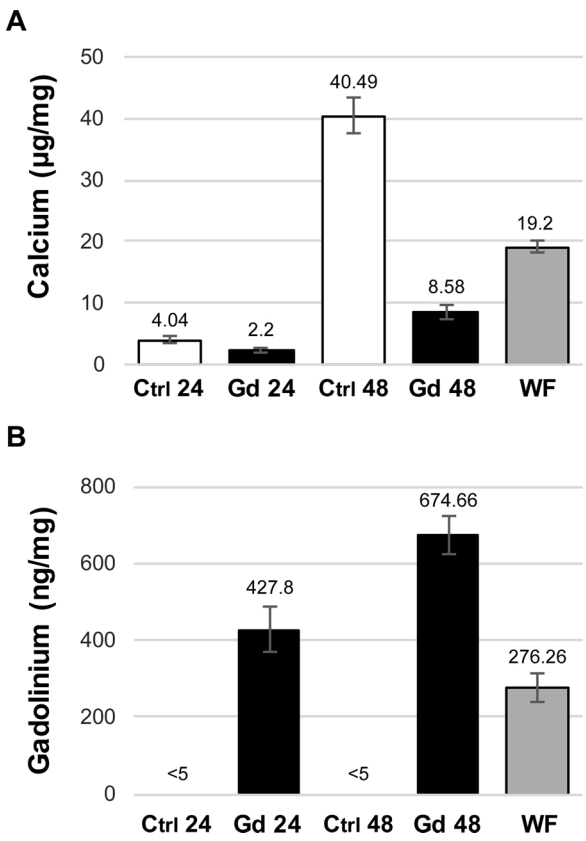

Fig. 2. Total Ca (A) and Gd (B) content determined by Flame Atomic Absorption Spectrometry at 24 and 48 hpf in *P. lividus* embryos: Ctrl 24 and Ctrl 48, controls at 24 and 48 hpf; Gd 24 and Gd 48, 20 µM Gd-exposed embryos at 24 and 48 hpf; WF, Washed Free embryos. Bars represent mean (N = 3) ± SD of embryo from the three separate fertilizations.

3.3.1. *P. lividus*

3.3.1.1. Early expressed genes: alx-1, nodal. Fig. 4 shows the mRNA levels in *P. lividus* embryos exposed to 20 µM Gd after 6, 24 and 48 h of development, in comparison to controls (unexposed embryos) at the same larval stage. The histogram in Fig. 4A shows the relative quantity of *alx-1* and *nodal* transcripts. At 6 hpf there was a significant 38% (± 0.02 SD) and 29% (± 0.03 SD) decrease in the relative transcription levels of *alx-1* and *nodal* compared to controls, respectively. At 24 hpf, *alx-1* and *nodal* show, respectively, 43% (± 0.07 SD) and 59% (± 0.05 SD) reduction of their relative transcriptional levels (Fig. 4A). At 48 hpf, *nodal* expression showed a 20% (± 0.08 SD) reduction, while *alx-1* expression was significantly reduced, being 57% (± 0.06 SD) less than controls (Fig. 4A). The pair-wise tests (Tukey HSD, Table S1), revealed that all these differences were significant ($P < 0.05$), except for *nodal* at 48 hpf (Fig. 4A and Table S1).

3.3.1.2. Signaling molecules genes: univin, vegf, vegf-r, fgf. The *vegf* and *vegf-r* mRNAs levels were not significantly different to those of controls, suggesting that expression of these signaling molecules genes is not affected by Gd-exposure (Fig. 4B and Table S1). A significant ($P < 0.05$, Table S1) down-regulation of *univin* and *fgf* transcripts was observed at 48 hpf, with reduced levels of 48% (± 0.05 SD) and 58% (± 0.04 SD), respectively, while no significant difference was detected at 24 hpf (Fig. 4B).

3.3.1.3. Skeletal genes: msp130, p16, p19. While no change in the expression levels of *msp130* was detected at 24 hpf, we found a significant ($P < 0.05$, Table S1) 28% (± 0.05 SD) reduction and 35% (± 0.08 SD) increase for *p16* and *p19*, respectively. At 48 hpf, there was a significant ($P < 0.05$, Table S1) 52% (± 0.12 SD) and 49% (± 0.06 SD) reduction for *msp130* and *p16,* respectively, and a 23% (± 0.05 SD) reduction for *p19* (Fig. 4C).

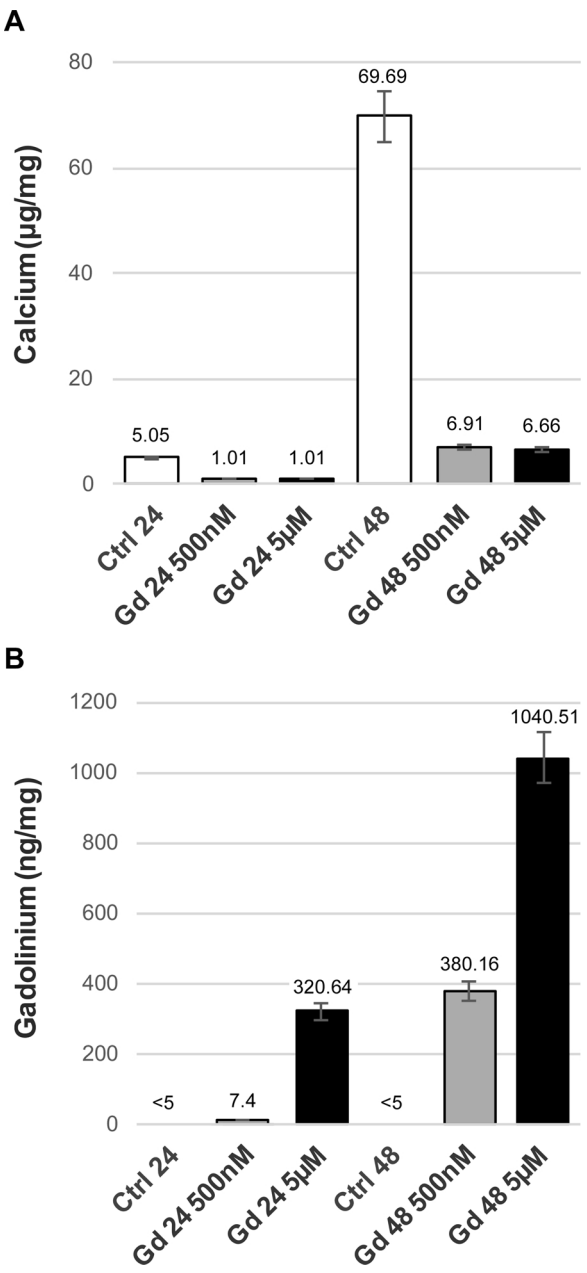

Fig. 3. Total Ca (A) and Gd (B) content determined by Flame Atomic Absorption Spectrometry at 24 and 48 hpf in *H. tuberculata* embryos: Ctrl 24 and Ctrl 48, controls at 24 and 48 hpf; Gd 24 and Gd 48, 500 nM and 5 µM Gd-exposed embryos at 24 and 48 hpf. Bars represent mean (N = 3) ± SD of embryo from the three separate fertilizations.

3.3.2. *H. tuberculata*

3.3.2.1. Early expressed genes: nodal, lefty, bmp. Expression levels of *nodal, lefty* and *bmp* were significantly ($P < 0.05$, Table S1) reduced after 24 h of exposure to both 500 nM and 5 µM Gd (Fig. 5A). A 33% decrease in *nodal* expression was observed in embryos exposed for 24 h to 500 nM (± 0.01 SD) and 5 µM (± 0.04 SD) Gd, while a significant 20% (± 0.005 SD) reduction was observed at 48 hpf only at the highest dose (5 µM). A 29% (± 0.04 SD) and 43% (± 0.11 SD) decrease in *lefty* expression was observed in embryos exposed for 24 h to 500 nM and 5 µM Gd, respectively. A significant 19% (± 0.05 SD) and 29% (± 0.09 SD) decrease in *bmp* expression was observed in embryos

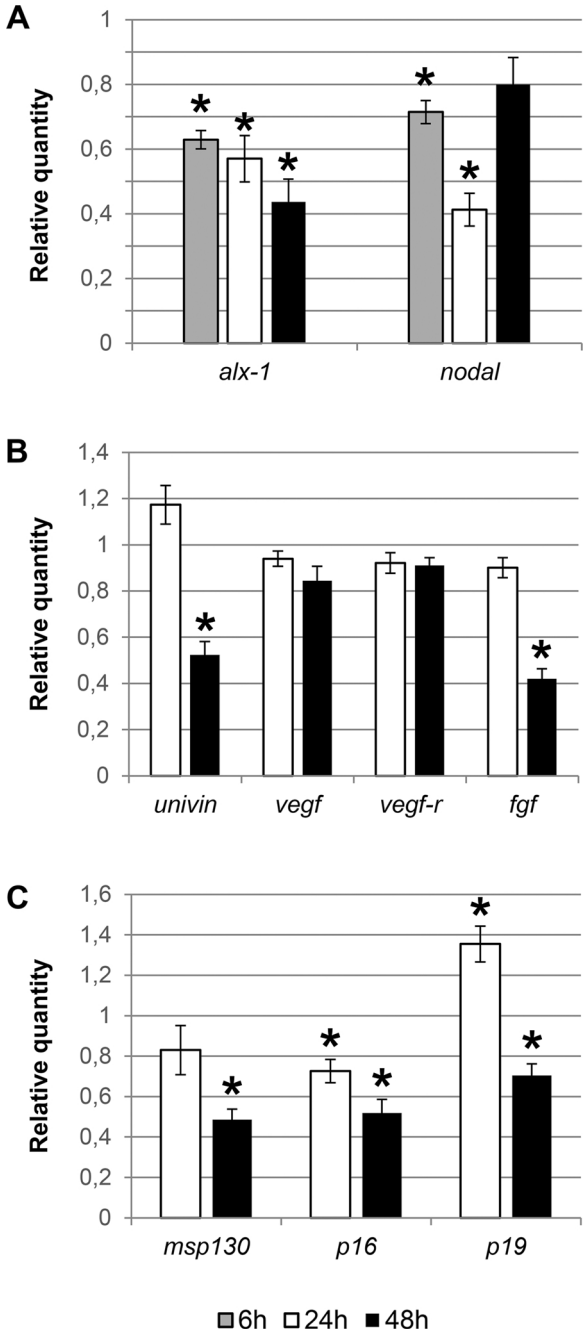

Fig. 4. Relative expression of: (A) *alx-1, nodal;* (B) *univin, vegf, vegf-r, fgf;* (C) *msp130, p16* and *p19,* in Gd-exposed *P. lividus* embryos. Histograms show the relative analysis of One Step RT-PCR products. Mean relative levels are expressed in arbitrary units as fold change compared to the control sample, assumed as 1 in the histogram, using the endogenous gene *Pl*-S24 for normalization. Bars represent mean (N = 9, see methods ± SD), and asterisks indicate responses that are significantly different from the controls (*P < 0.05).

exposed for 24 h to 500 nM and 5 µM Gd, respectively. No significant changes were detected at 48 hpf in *bmp* and *lefty* expression at either concentration.

3.3.2.2. Signalling molecule genes: fgf, vegf. The *fgf* had a significant 24% (± 0.03 SD) and 19% (± 0.08 SD) reduction in embryos exposed for 24 h to 500 nM and 5 µM Gd, respectively, and a 20% (± 0.10 SD) and 30% (± 0.09 SD) reduction in embryos exposed for 48 h to 500 nM and 5 µM Gd, respectively (Fig. 5B). The *vegf* expression was significantly up-regulated at 24 hpf, with a 2-fold increase (± 0.01 SD) of the mRNA levels at 500 nM and a 2.79-fold increase (± 0.06 SD) at 5 µM Gd,

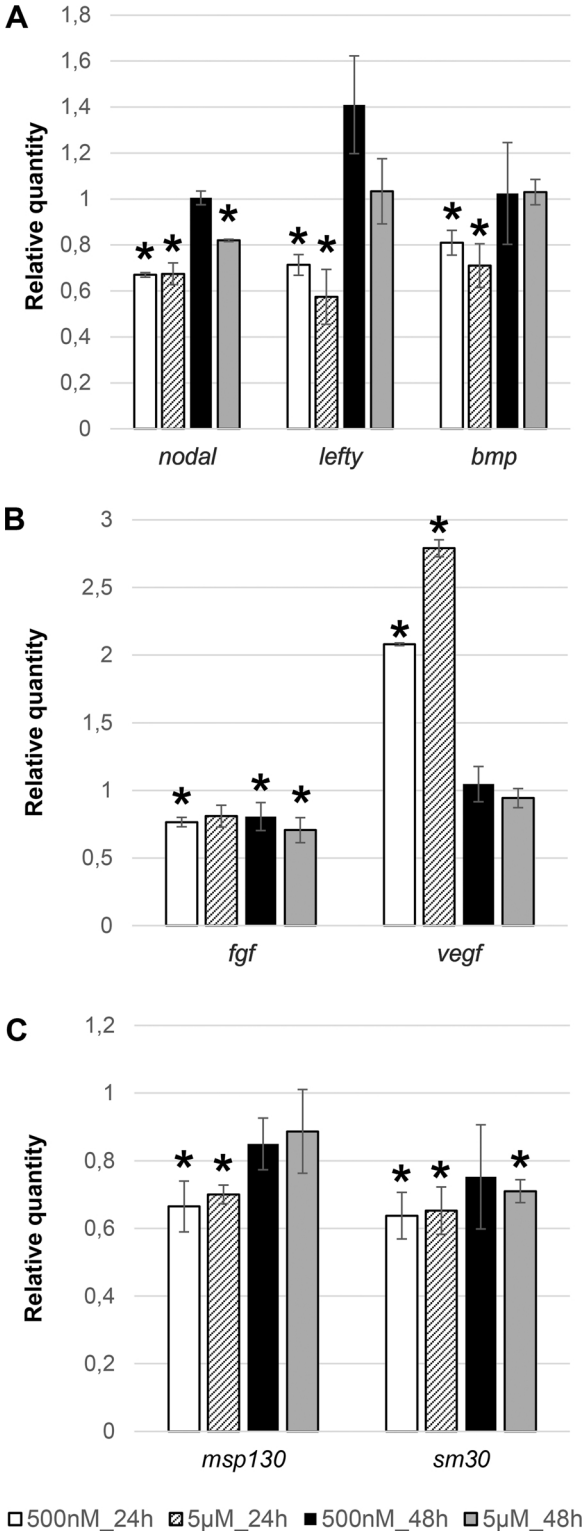

Fig. 5. Relative expression of: (A) *nodal, lefty, bmp;* (B) *vegf, fgf;* (C) *msp130* and *sm30,* in Gd-exposed *H. tuberculata* embryos. Histograms show the relative analysis of One Step RT-PCR products. Mean relative levels are expressed in arbitrary units as fold change compared to the control sample, assumed as 1 in the histogram, using the endogenous gene *Ht*-Z12 for normalization. Bars represent mean (N = 9, see methods ± SD), and asterisks indicate responses that are significantly different from the controls (*P < 0.05).

while at 48 hpf the transcription levels did not differ from that in controls (Table S1).

3.3.2.3. Skeletal genes: msp130, sm30. We found a significant 34%

(± 0.07 SD) and 30% (± 0.02 SD) reduction in the mRNA levels of *msp130* in embryos exposed for 24 h to 500 nM and 5 μM Gd, respectively, while at 48 hpf the transcription levels did not differ from that in controls (Fig. 5C and Table S1). A significant 37% (± 0.06 SD) and 35% (± 0.06 SD) decrease in *sm30* expression was observed in embryos exposed for 24 h to 500 nM and 5 μM Gd, respectively, while a significant 29% (± 0.03 SD) decrease was detected at 48 hpf only at the highest concentration (Fig. 5C and Table S1).

4. Discussion

Gd is receiving increased attention within the framework of risk assessment studies with pollutants of emerging concern due to its frequent detection in aquatic and marine environments (Bau and Dulski, 1996; Nozaki et al., 2000; Elbaz-Poulichet et al., 2002; Zhu et al., 2004; Ogata and Terakado, 2006; Kulaksiz and Bau, 2007; Hatje et al., 2016). The present study investigated whether Gd interferes with development of two sea urchin species, the Mediterranean *P. lividus*, and the Australian *H. tuberculata*. This agent induces morphological malformations and altered expression of genes associated with skeletogenesis. Gd exposure has a negative effect on skeleton development with a similar morphological response in the two species, implying a similar mechanism underlying abnormal skeletogenesis.

The developmental success of sea urchin larvae depends on their swimming and feeding ability which is determined by arm length (Strathmann et al., 1992; Allen, 2008; Soars et al., 2009) and so it is likely that Gd exposure would reduce survival in nature. Several studies suggested that Gd^{3+} ion concentrations in the micromolar range (between 1 and 200 μM) can block calcium channels in *Xenopus* oocytes (Yang and Sachs, 1989), in the membrane of sea urchin eggs (David et al., 1988), and in mammalian cell lines (Broad et al., 1999; Lansman, 1990; Luo et al., 2001). Thus, the disruption of spicule formation is likely to be due to the action of Gd^{3+} as a blocker of calcium channels. Our results on the Ca and Gd content of larvae obtained by FAAS showed a reduction in the Ca amount in parallel with an increase in the Gd content, likely due to Gd interference with calcium uptake and directly affecting biomineral formation. Strikingly, we found an important decrease in Ca content also in embryos exposed to a Gd concentration in the nanomolar range (*H. tuberculata* exposed to 500 nM Gd). Thus, it appears that Gd^{3+} competes with Ca^{2+} for binding to the calcium channels. As a trivalent ion, Gd^{3+} binds with much higher affinity (Sherry et al., 2009). Here we showed that this agent accumulated in embryos and larvae in a time- and concentration-dependent manner. Interestingly, other aspects of development such as ectoderm and endoderm differentiation did not appear to be affected by Gd.

In WF embryos skeleton growth partially recovered. The larvae had longer spicules than those continuously exposed to Gd for 48 h, but the skeleton pattern was abnormal. During the 24 h rescue period, it is likely that the uptake of Ca was reinitiated, as indicated by the higher levels of Ca in these embryos than in those continuously exposed to Gd for 48 h. These WF embryos were thus able to resume skeleton elongation. However, they were not able to extend their spicules with the correct skeleton pattern and they had the same aberrant morphotypes as seen in embryos continuously exposed to Gd. If the limited availability of calcium is the major obstacle to spicule elongation, then why is the skeleton pattern strongly perturbed in Gd-exposed embryos as well as in WF embryos? Significant insights emerged from our analysis of genes involved in the gene regulatory network (GRN) that underlies the development of the sea urchin larval endoskeleton in response to Gd treatment. Metals have long been used to perturb sea urchin skeletogenesis to provide insights into the basis of gene expression regulation controlling correct development (Hardin et al., 1992; Livingston and Wilt, 1989; Poustka et al., 2007; Timourian, 1968).

Alx1 is a gene encoding a key transcription factor expressed selectively in the large micromere lineage and essential for PMC specification (Ettensohn et al., 2003). As *alx-1* is one of the essential regulators acting upstream in the skeletogenic GRN triggering the cascade of events leading to expression of downstream structural genes, reduced levels of this gene in treated *P. lividus* embryos at 6, 24 (38 and 43% reduction respectively) and 48 h (57% reduction) may have caused a flow on effect of reduced gene expression at 48 hpf of the downstream genes (Garfield et al., 2013), specifically for *msp130*, which encodes a PMC-specific cell surface glycoprotein (Leaf et al., 1987) and *p16* and *p19* which encode biomineralization acidic proteins with a hypothesized role in spicule elongation for p16 and growth of the spicule girth for p19 (Costa et al., 2012).

Nodal has been extensively investigated in sea urchin development, having a key role during morphogenesis. The Nodal-Lefty-Pitx2 signaling pathway regulates the establishment of both the left-right asymmetry and the oral-aboral polarity during development of the sea urchin embryo (Duboc et al., 2005; Koop et al., 2017). The maximal reduction of *nodal* expression was observed in both species at 24 hpf, the crucial moment when Nodal starts acting for the establishment of the left-right asymmetry (Duboc et al., 2005). This indicates that the observed reduced transcriptional levels of *nodal* at 24 hpf might be critical for the left-right larval symmetry, and this gene is probably involved in the asymmetrical spicule growth in Gd-exposed embryos.

Establishment of left-right asymmetry in sea urchin embryos involves reciprocal signaling between the ectoderm expressing *nodal* and a left-right organizer of endodermal origin and requires several signaling pathways including the *notch, fgf-erk, bmp2/4* and *univin/vg1* (Bessodes et al., 2012). The *vegf* and *fgf* pathways are also essential to provide guidance and differentiation cues to primary mesenchyme cells (PMCs) during sea urchin gastrulation, controlling the directional migration of PMCs and the formation of the embryonic skeleton (Duloquin et al., 2007; Röttinger et al., 2008). The down-regulation of *fgf* expression in *P. lividus* Gd-exposed embryos at 48 hpf may have inhibited spicule elongation. On the other hand, the down-regulation of *fgf* observed at 24 hpf and the great up-regulation of *vegf* in *H. tuberculata* Gd-exposed embryos may result in abnormal and excessive branching of the skeleton, as observed in many embryos.

Cavalieri et al. (2011) suggested that the gene *strim1* is probably not required for PMCs specification but it is necessary for proper positioning of PMCs in the blastocoel, and that *strim1* indirectly participates in the transcription of the *fgfA* gene to achieve the maximum expression in ectoderm cells that is essential for turning on the expression of terminal differentiation genes, such as *sm30* (Cavalieri et al., 2011). It is interesting to note that the Strim1 protein needs calcium ions to work properly. Thus, the lack of Ca in Gd-exposed embryos could provoke the abnormal functioning of Ca^{2+}-dependent proteins such as Strim1 and the misexpression of the genes requiring its regulatory activity, i.e. *fgfA* and *sm30*.

Development of the sea urchin larval skeleton requires a complex genomic regulatory program that has been conserved over millions of years (Davidson and Erwin, 2006), although levels of expression may differ between phylogenetically distant species (Kalinka et al., 2010; Irie and Kuratani, 2011). Thus, the differences in gene expression in response to Gd treatment in *P. lividus* and *H. tuberculata* are not surprising, despite their similar phenotypic response to this agent. These species of sea urchin have contrasting investment in skeleton production: *H. tuberculata* produces robust extensive skeleton with fenestrated arm rods, typical of the Echinometridae (Kinjo et al., 2008), while *P. lividus* produces elongated and thin unfenestrated rods, typical of the Echinidae (Emlet, 1982). This difference is likely to be associated with different levels of calcium uptake and expression of skeleton specific transcripts. Strikingly, *H. tuberculata* control larvae have a higher amount of calcium at 48 hpf (69.69 μg/mg ± 3.48 SD) than *P. lividus* larvae at the same stage (40.49 μg/mg ± 3 SD), reflecting the construction of a more robust skeleton structure. Thus, *H. tuberculata* embryos may require higher levels of *fgf* by 24 hto support skeleton growth. In addition, some *H. tuberculata* Gd-exposed embryos had skeletons that were more branched than in controls. It is known that

vegf is involved in spiculogenesis and that its concentration controls the spicules shape and their branching (Knapp et al., 2012). So, the comparatively higher increase in the *vegf* mRNA levels at 24 h in *H. tuberculata* Gd-exposed embryos may be the cause for the increased branching of the spicules in these embryos.

Due to the fabrication of a more extensive skeleton, *H. tuberculata* may have higher endogenous levels of proteins involved in skeleton formation than *P. lividus*, and this could explain why we found higher levels of *msp130* at 48 hpf in *H. tuberculata* Gd-exposed embryos than in *P. lividus* Gd-exposed embryos. Similar implications were suggested in a recent work that compared the effects of acetazolamide on carbonic anhydrase activity in these two species (Zito et al., 2015).

5. Conclusions

Pollution due to the continuous introduction of human-derived contaminants in the marine environment poses a threat to marine species worldwide. Chemical pollutants represent a constant source of evolutionary challenges for living organisms, strenuously challenging their adaptive potential (Whitehead, 2014). Phenotypic responses to environmental changes may be a key factor for the survival of a species, by buffering developmental processes via altered morphology, gene expression, or stress response mechanisms (Williams et al., 2008; Chiarelli et al., 2016). Key findings on the variable sensitivity of early life stages of different sea urchin species highlight the importance of testing the effects of pollution for risk assessment in several species, even within the same taxonomic group (Saitoh et al., 2010; Burić et al., 2015; Martino et al., 2017a).

Here we show the harmful effects of Gd exposure on the development of two geographically and phylogenetically distant sea urchin species, *P. lividus* and *H. tuberculata*. The phenotypic response mainly affected skeleton growth. We found a misregulation of the skeletogenic GRN in both species but, strikingly, with species-specific differences. Comparing the gene expression changes within a specific cell lineage after Gd exposure among different species can provide insights for evolutionary questions to understand how these differences are generated, and for ecotoxicological questions, to address how such differences influence the sensitivity to environmental pollution. Comparative gene expression analysis can thus provide some valuable insights to understand the impact of regulatory changes on the development of differences in specific structures such as the larval skeleton of *P. lividus* and *H. tuberculata* and the potential mechanisms by which toxic agents such as Gd operate at the genetic and cellular level.

Funding

This research has been supported by a PhD grant to CM from Dept. STEBICEF, University of Palermo [grant number: D50002D15 + 1001], by a NSW Environmental Trust grant [grant number: RD09] to MB, and by the DeCroMed Project [EU-Research & Innovation Strategy, Regione Sicilia- PO-FESR 2007-2013, CUP: G93F12000190007] to Valeria Matranga.

Author contributions

Conceived and designed the experiments: CM, CC, MCR, MB. Performed the experiments: CM, CC, DK. Performed statistical analysis: CM. Performed FAAS analysis: RS. Analyzed the data: CM, CC, DK, MCR, MB. Wrote the paper: CM, MB. Revised the manuscript: CC, MCR, MB.

Declaration of interest

The authors declare no conflict of interest.

Acknowledgements

This work is dedicated to the memory of Valeria Matranga, our great colleague and scientist. The authors thank: Dr. Vincenzo Cavalieri (Dept. STEBICEF, University of Palermo) for kindly providing the primers for Pl-nodal and Pl-fgf and for the fruitful discussions; Prof. Matteo Cammarata (Dept. STEBICEF, University of Palermo) for his help with the statistical analysis; Mr. Mauro Biondo (IBIM-CNR) for his technical assistance; Dr. Marco Trifuoggi (Dept. Chemical Sciences, University of Naples Federico II) for his help with the FAAS analysis. This is contribution number 216 of the Sydney Institute of Marine Science.

Appendix A. Supplementary data

Supplementary data associated with this article can be found, in the online version, at http://dx.doi.org/10.1016/j.aquatox.2017.11.004.

References

Agnello, M., Chiarelli, R., Martino, C., Bosco, L., Roccheri, M.C., 2016. Autophagy is required for sea urchin oogenesis and early development. Zygote 24 (6), 918–926. http://dx.doi.org/10.1017/S0967199416000253.

Allen, J.D., 2008. Size-specific predation on marine invertebrate larvae. Biol. Bull. 214, 42–49. http://dx.doi.org/10.2307/25066658.

Antiabong, J.F., Ngoepe, M.G., Abechi, A.S., 2016. Semi-quantitative digital analysis of polymerase chain reaction-electrophoresis gel: potential applications in low-income veterinary laboratories. Vet. World 9 (9), 935–939. http://dx.doi.org/10.14202/vetworld.2016.935-939.

Bau, M., Dulski, P., 1996. Anthropogenic origin of positive gadolinium anomalies in river waters. Earth Planet. Sci. Lett. 143 (1-4), 245–255.

Berninger, J.P., Brooks, B.W., 2010. Leveraging mammalian pharmaceutical toxicology and pharmacology data to predict chronic fish responses to pharmaceuticals. Toxicol. Lett. 193, 69–78. http://dx.doi.org/10.1016/j.toxlet.2009.12.006.

Bessodes, N., Haillot, E., Duboc, V., Röttinger, E., Lahaye, F., Lepage, T., 2012. Reciprocal signaling between the ectoderm and a mesendodermal left-right organizer directs left-right determination in the sea urchin embryo. PLoS Genet. 8, e1003121. http://dx.doi.org/10.1371/journal.pgen.1003121.

Bonaventura, R., Matranga, V., 2017. Overview of the molecular defense systems used by sea urchin embryos to cope with UV radiation. Mar. Environ. Res. 128, 25–35. http://dx.doi.org/10.1016/j.marenvres.2016.05.019.

Bonaventura, R., Poma, V., Costa, C., Matranga, V., 2005. UVB radiation prevents skeleton growth and stimulates the expression of stress markers in sea urchin embryos. Biochem. Biophys. Res. Commun. 328, 150–157. http://dx.doi.org/10.1016/j.bbrc.2004.12.161.

Boxall, A.B., Rudd, M.A., Brooks, B.W., Caldwell, D.J., Choi, K., Hickmann, S., Innes, E., Ostapyk, K., Staveley, J.P., Verslycke, T., Ankley, G.T., Beazley, K.F., Belanger, S.E., Berninger, J.P., Carriquiriborde, P., Coors, A., Deleo, P.C., Dyer, S.D., Ericson, J.F., Gagné, F., Giesy, J.P., Gouin, T., Hallstrom, L., Karlsson, M.V., Larsson, D.G., Lazorchak, J.M., Mastrocco, F., McLaughlin, A., McMaster, M.E., Meyerhoff, R.D., Moore, R., Parrott, J.L., Snape, J.R., Murray-Smith, R., Servos, M.R., Sibley, P.K., Straub, J.O., Szabo, N.D., Topp, E., Tetreault, G.R., Trudeau, V.L., Van Der Kraak, G., 2012. Pharmaceuticals and personal care products in the environment: what are the big questions? Environ. Health Perspect. 120, 1221–1229. http://dx.doi.org/10.1289/ehp.1104477.

Brausch, J.M., Connors, K.A., Brooks, B.W., Rand, G.M., 2012. Human pharmaceuticals in the aquatic environment: a review of recent toxicological studies and considerations for toxicity testing. Rev. Environ. Contam. Toxicol. 218, 1–99. http://dx.doi.org/10.1007/978-1-4614-3137-4_1.

Broad, L.M., Cannon, T.R., Taylor, C.W., 1999. A non-capacitative pathway activated by arachidonic acid is the major Ca^{2+} entry mechanism in rat A7r5 smooth muscle cells stimulated with low concentrations of vasopressin. J. Physiol. 517, 121e134.

Brooks, B.W., Huggett, D.B., 2012. Human Pharmaceuticals in the Environment: Current and Future Perspectives. Springer, New York. http://dx.doi.org/10.1007/978-1-4614-3473-3.

Burić, P., Jaksić, Z., Stajner, L., Dutour Sikirić, M., Jurasin, D., Cascio, C., Calzolai, L., Lyons, D.M., 2015. Effect of silver nanoparticles on Mediterranean sea urchin embryonal development is species specific and depends on moment of first exposure. Mar. Env. Res. 111, 50–59. http://dx.doi.org/10.1016/j.marenvres.2015.06.015.

Byrne, M., Lamare, M., Winter, D., Dworjanyn, S.A., Uthicke, S., 2013. The stunting effect of a high CO2 ocean on calcification and development in sea urchin larvae, a synthesis from the tropics to the poles. Philos. Trans. R. Soc. Lond. B Biol. Sci. 368, 20120439. http://dx.doi.org/10.1098/rstb.2012.0439.

Cavalieri, V., Spinelli, G., 2014. Early asymmetric cues triggering the dorsal/ventral gene regulatory network of the sea urchin embryo. Elife 3, e04664. http://dx.doi.org/10.7554/eLife.04664.

Cavalieri, V., Guarcello, R., Spinelli, G., 2011. Specific expression of a TRIM-containing factor in ectoderm cells affects the skeletal morphogenetic program of the sea urchin embryo. Development 138, 4279–4290. http://dx.doi.org/10.1242/dev.066480.

Chen, Y., Cao, X.D., Lu, Y., Wang, X.R., 2000. Effects of rare earth metal ions and their EDTA complexes on antioxidant enzymes of fish liver. Bull. Environ. Contam.

Toxicol. 65, 357–365.
Chiarelli, R., Martino, C., Agnello, M., Bosco, L., Roccheri, M.C., 2016. Autophagy as a defense strategy against stress: focus on *Paracentrotus lividus* sea urchin embryos exposed to cadmium. Cell Stress Chaperones 21, 19–27. http://dx.doi.org/10.1007/s12192-015-0639-3.
Costa, C., Cavalcante, C., Zito, F., Yokota, Y., Matranga, V., 2010. Phylogenetic analysis and homology modelling of *Paracentrotus lividus* nectin. Mol. Divers. 14 (4), 653–665. http://dx.doi.org/10.1007/s11030-009-9203-3.
Costa, C., Karakostis, K., Zito, F., Matranga, V., 2012. Phylogenetic analysis and expression patterns of p16 and p19 in *Paracentrotus lividus* embryos. Dev. Genes Evol. 222, 245–251. http://dx.doi.org/10.1007/s00427-012-0405-9.
Cowper, S.E., Robin, H.S., Steinberg, S.M., Su, L.D., Gupta, S., LeBoit, P.E., 2000. Scleromyxoedema-like cutaneous diseases in renal-dialysis patients. Lancet 356, 1000–1001. http://dx.doi.org/10.1016/S0140-6736(00)02694-5.
David, C., Halliwell, J., Whitaker, M., 1988. Some properties of the membrane currents underlying the fertilization potential in sea urchin eggs. J. Physiol. 402, 139–154.
Davidson, E.H., Erwin, D.H., 2006. Gene regulatory networks and the evolution of animal body plans. Science 311, 796–800. http://dx.doi.org/10.1126/science.1113832.
Duboc, V., Röttinger, E., Lapraz, F., Besnardeau, L., Lepage, T., 2005. Left-right asymmetry in the sea urchin embryo is regulated by nodal signaling on the right side. Dev. Cell 9, 147–158. http://dx.doi.org/10.1016/j.devcel.2005.05.008.
Duloquin, L., Lhomond, G., Gache, C., 2007. Localized VEGF signaling from ectoderm to mesenchyme cells controls morphogenesis of the sea urchin embryo skeleton. Development 134, 2293–2302. http://dx.doi.org/10.1242/dev.005108.
Elbaz-Poulichet, F., Seidel, J.-L., Othoniel, C., 2002. Occurrence of an anthropogenic gadolinium anomaly in river and coastal waters of Southern France. Water Res. 36 (4), 1102–1105.
Emlet, R.B., 1982. Echinoderm calcite: a mechanical analysis from larval spicules. Biol. Bull. 163, 264–275.
Ettensohn, C.A., Illies, M.R., Oliveri, P., De Jong, D.L., 2003. Alx1, a member of the Cart1/Alx3/Alx4 subfamily of Paired-class homeodomain proteins, is an essential component of the gene network controlling skeletogenic fate specification in the sea urchin embryo. Development 130, 2917–2928.
Fong, P.P., Ford, A.T., 2014. The biological effects of antidepressants on the molluscs and crustaceans: a review. Aquat. Toxicol. 151, 4–13. http://dx.doi.org/10.1016/j.aquatox.2013.12.003.
Garfield, D.A., Runcie, D.E., Babbitt, C.C., Haygood, R., Nielsen, W.J., Wray, G.A., 2013. The impact of gene expression variation on the robustness and evolvability of a developmental gene regulatory network. PLoS Biol. 11 (10), e1001696. http://dx.doi.org/10.1371/journal.pbio.1001696.
Grobner, T., 2006. Gadolinium–a specific trigger for the development of nephrogenic fibrosing dermopathy and nephrogenic systemic fibrosis? Nephrol. Dial. Transplant. 21, 1104–1108. http://dx.doi.org/10.1093/ndt/gfk062.
Gunnarsson, L., Jauhiainen, A., Kristiansson, E., Nerman, O., Larsson, D.G., 2008. Evolutionary conservation of human drug targets in organisms used for environmental risk assessments. Environ. Sci. Technol. 42, 5807–5813.
Hanana, H., Turcotte, P., André, C., Gagnon, C., Gagné, F., 2017. Comparative study of the effects of gadolinium chloride and gadolinium − based magnetic resonance imaging contrast agent on freshwater mussel, *Dreissena polymorpha*. Chemosphere 181, 197–207. http://dx.doi.org/10.1016/j.chemosphere.2017.04.073.
Hardin, J., Coffman, J.A., Black, S.D., McClay, D.R., 1992. Commitment along the dorsoventral axis of the sea urchin embryo is altered in response to NiCl2. Development 116, 671–685.
Hatje, V., Bruland, K.W., Flegal, A.R., 2016. Increases in Anthropogenic Gadolinium Anomalies and Rare Earth Element Concentrations in San Francisco Bay over a 20 Year Record. Environ. Sci. Technol. 50, 4159–4168. http://dx.doi.org/10.1021/acs.est.5b04322.
Irie, N., Kuratani, S., 2011. Comparative transcriptome analysis reveals vertebrate phylotypic period during organogenesis. Nat. Commun. 2, 248. http://dx.doi.org/10.1038/ncomms1248.
Joffe, P., Thomsen, H.S., Meusel, M., 1998. Pharmacokinetics of gadodiamide injection in patients with severe renal insufficiency and patients undergoing hemodialysis or continuous ambulatory peritoneal dialysis. Acad. Radiol. 5, 491–502.
Kalinka, A.T., Varga, K.M., Gerrard, D.T., Preibisch, S., Corcoran, D.L., Jarrells, J., Ohler, U., Bergman, C.M., Tomancak, P., 2010. Gene expression divergence recapitulates the developmental hourglass model. Nature 468, 811–814. http://dx.doi.org/10.1038/nature09634.
Kinjo, S., Shirayama, Y., Wada, H., 2008. Evolutionary history of larval skeletal morphology in sea urchin Echinometridae (Echinoidea: echinodermata) as deduced from mitochondrial DNA molecular phylogeny. Evol. Dev. 10, 632–641. http://dx.doi.org/10.1111/j.1525-142X.2008.00277.x.
Knapp, R.T., Wu, C.H., Mobilia, K.C., Joester, D., 2012. Recombinant sea urchin vascular endothelial growth factor directs single-crystal growth and branching in vitro. J. Am. Chem. Soc. 134, 17908–17911. http://dx.doi.org/10.1021/ja309024b.
Koop, D., Cisternas, P., Morris, V.B., Strbenac, D., Yang, J.Y.H., Wray, G.A., Byrne, M., 2017. Nodal and BMP expression during the transition to pentamery in the sea urchin Heliocidaris erytrogramma: insight into patterning the enigmatic echinoderm body plan. BMC Dev. Biol. 17, 4. http://dx.doi.org/10.1186/s12861-017-0145-1.
Kulaksiz, S., Bau, M., 2007. Contrasting behaviour of anthropogenic gadolinium and natural rare earth elements in estuaries and the gadolinium input into the North Sea. Earth Planet. Sci. Lett. 260 (1–2), 361–371.
Lansman, J.B., 1990. Blockade of current through single calcium channels by triva- lent lanthanide cations: effect of ionic radius on the rates of ion entry and exit. J. Gen. Physiol. 95, 679–696.
Laville, N., Aït-Aïssa, S., Gomez, E., Casellas, C., Porcher, J.M., 2004. Effects of human pharmaceuticals on cytotoxicity, EROD activity and ROS production in fish hepatocytes. Toxicology 196, 41–55. http://dx.doi.org/10.1016/j.tox.2003.11.002.
Lawrence, J.M., 2013. Sea Urchins: Biology and Ecology, third ed. Elsevier, London.
Leaf, D.S., Anstrom, J.A., Chin, J.E., Harkey, M.A., 1987. Antibodies to a fusion protein identify a cDNA clone encoding msp130, a primary mesenchyme-specific cell surface protein of the sea urchin embryo. Dev. Biol. 121, 29–40.
Lide, D.R., Haynes, W.M.M., Baysinger, G., Berger, L.I., Roth, D.L., Zwillinger, D., Frenkel, M., Goldberg, R.N., 2009. CRC Handbook of Chemistry and Physics, 90th ed. CRC Press (Taylor and Francis group), Boca Raton, FL.
Livingston, B.T., Wilt, F.H., 1989. Lithium evokes expression of vegetal-specific molecules in the animal blastomeres of sea urchin embryos. Proc. Natl. Acad. Sci. U. S. A. 86, 3669–3673.
Luo, D., Broad, L.M., Bird, G.S.J., Putney Jr., J.W., 2001. Signaling pathways underlying muscarinic receptor-induced $[Ca^{2+}]_i$ oscillations in HEK293 cells. J. Biol. Chem. 276, 5613–5621.
Martino, C., Bonaventura, R., Byrne, M., Roccheri, M., Matranga, V., 2017a. Effects of exposure to gadolinium on the development of geographically and phylogenetically distant sea urchins species. Mar. Environ. Res. 128, 98–106. http://dx.doi.org/10.1016/j.marenvres.2016.06.001.
Martino, C., Chiarelli, R., Bosco, L., Roccheri, M.C., 2017b. Induction of skeletal abnormalities and autophagy in *Paracentrotus lividus* sea urchin embryos exposed to gadolinium. Mar. Environ. Res. 130, 12–20. http://dx.doi.org/10.1016/j.marenvres.2017.07.007.
Matranga, V., Zito, F., Costa, C., Bonaventura, R., Giarrusso, S., Celi, F., 2010. Embryonic development and skeletogenic gene expression affected by X-rays in the Mediterranean sea urchin *Paracentrotus lividus*. Ecotoxicology 19, 530–537. http://dx.doi.org/10.1007/s10646-009-0444-9.
Matranga, V., Bonaventura, R., Costa, C., Karakostis, K., Pinsino, A., Russo, R., Zito, F., 2011. Echinoderms as blueprints for biocalcification: regulation of skeletogenic genes and matrices. Prog. Mol. Subcell. Biol. 52, 225–248. http://dx.doi.org/10.1007/978-3-642-21230-7_8.
Matranga, V., Pinsino, A., Bonaventura, R., Costa, C., Karakostis, K., Martino, C., Russo, R., Zito, F., 2013. Cellular and molecular bases of biomineralization in sea urchin embryos. Cah. Biol. Mar. 54, 467–478.
Mlinar, B., Enyeart, J.J., 1993. Block of current through T-type calcium channels by trivalent metal cations and nickel in neural rat and human cells. J. Physiol. 469, 639–652.
Niendorf, H.P., Haustein, J., Cornelius, I., Alhassan, A., Clauss, W., 1991. Safety of gadolinium-DTPA: extended clinical experience. Magn. Reson. Med. 22, 222–232.
Nozaki, Y., Lerche, D., Alibo, D.S., Tsutsumi, M., 2000. Dissolved indium and rare earth elements in three Japanese rivers and Tokyo Bay: evidence for anthropogenic Gd. Geochim. Cosmochim. Acta 64 (23), 39753982.
Ogata, T., Terakado, Y., 2006. Rare earth element abundances in some seawaters and related river waters from the Osaka Bay area, Japan: significance of anthropo- genic Gd. Geochem. J. 40 (5), 463–474.
Oliveri, P., Tu, Q., Davidson, E.H., 2008. Global regulatory logic for specification of an embryonic cell lineage. Proc. Natl. Acad. Sci. U. S. A. 105, 5955–5962. http://dx.doi.org/10.1073/pnas.0711220105.
Pinsino, A., Roccheri, M.C., Costa, C., Matranga, V., 2011. Manganese interferes with calcium, perturbs ERK signaling, and produces embryos with no skeleton. Toxicol. Sci. 123, 217–230. http://dx.doi.org/10.1093/toxsci/kfr152.
Poustka, A.J., Kühn, A., Groth, D., Weise, V., Yaguchi, S., Burke, R.D., Herwig, R., Lehrach, H., Panopoulou, G., 2007. A global view of gene expression in lithium and zinc treated sea urchin embryos: new components of gene regulatory networks. Genome Biol. 8, R85. http://dx.doi.org/10.1186/gb-2007-8-5-r85.
Röttinger, E., Saudemont, A., Duboc, V., Besnardeau, L., McClay, D., Lepage, T., 2008. FGF signals guide migration of mesenchymal cells, control skeletal morphogenesis [corrected] and regulate gastrulation during sea urchin development. Development 135, 353–365. http://dx.doi.org/10.1242/dev.014282.
Ragusa, M.A., Costa, S., Gianguzza, M., Roccheri, M.C., Gianguzza, F., 2013. Effects of cadmium exposure on sea urchin development assessed by SSH and RT-qPCR: metallothionein genes and their differential induction. Mol. Biol. Rep. 40, 2157–2167. http://dx.doi.org/10.1007/s11033-012-2275-7.
Ragusa, M.A., Costa, S., Cuttitta, A., Gianguzza, F., Nicosia, A., 2017. Coexposure to sulfamethoxazole and cadmium impairs development and attenuates transcriptional response in sea urchin embryo. Chemosphere 180, 275–284. http://dx.doi.org/10.1016/j.chemosphere.2017.04.030.
Russo, R., Bonaventura, R., Zito, F., Schröder, H.C., Müller, I., Müller, W.E., Matranga, V., 2003. Stress to cadmium monitored by metallothionein gene induction in *Paracentrotus lividus* embryos. Cell Stress Chaperones 8, 232–241.
Russo, R., Zito, F., Costa, C., Bonaventura, R., Matranga, V., 2010. Transcriptional increase and misexpression of 14-3-3 epsilon in sea urchin embryos exposed to UV-B. Cell Stress Chaperones 15, 993–1001. http://dx.doi.org/10.1007/s12192-010-0210-1.
Saitoh, M., Kuroda, R., Muranaka, Y., Uto, N., Murai, J., Kuroda, H., 2010. Asymmetric inhibition of spicule formation in sea urchin embryos with low concentrations of gadolinium ion. Dev. Growth Differ. 52 (9), 735–746. http://dx.doi.org/10.1111/j.1440-169X.2010.01210.x.
Sgroi, A., Colombo, P., Duro, G., Fried, M., Izzo, V., Giudice, G., 1996. cDNA sequence analysis and expression of the expression of the ribosomal protein S24 during oogenesis and embryonic development of the sea urchin *Paracentrotus lividus*. Biochem. Biophys. Res. Commun. 221, 361–367.
Sherry, A.D., Caravan, P., Lenkinski, R.E., 2009. Primer on gadolinium chemistry. J. Magn. Reson. Imag. 30, 1240–1248. http://dx.doi.org/10.1002/jmri.21966.
Soars, N.A., Prowse, T.A.A., Byrne, M., 2009. Overview of phenotypic plasticity in echinoid larvae, Echinopluteus transversus' type versus typical echinoplutei. Mar. Ecol. Prog. Ser. 383, 113–125. http://dx.doi.org/10.3354/meps07848.

Strathmann, R.R., Fenaux, L., Strathmann, M.F., 1992. Heterochronic developmental plasticity in larval sea-urchins and its implications for evolution of nonfeeding larvae. Evolution 46, 972–986.

Telgmann, L., Sperling, M., Karst, U., 2013. Determination of gadolinium-based MRI contrast agents in biological and environmental samples: a review. Anal. Chim. Acta 764, 1–16. http://dx.doi.org/10.1016/j.aca.2012.12.007.

Tellis, M.S., Lauer, M.M., Nadella, S., Bianchini, A., Wood, C.M., 2014. Sublethal mechanisms of Pb and Zn toxicity to the purple sea urchin (*Strongylocentrotus purpuratus*) during early development. Aquat. Toxicol. 146, 220–229. http://dx.doi.org/10.1016/j.aquatox.2013.11.004.

Timourian, H., 1968. The effect of zinc on sea urchin morphogenesis. J. Exp. Zool. 169, 121–132.

Tiwari, B., Sellamuthu, B., Ouarda, Y., Drogui, P., Tyagi, R.D., Buelna, G., 2017. Review on fate and mechanism of removal of pharmaceutical pollutants from wastewater using biological approach. Bioresour. Technol. 224, 1–12. http://dx.doi.org/10.1016/j.biortech.2016.11.042.

Vidavsky, N., Addadi, S., Schertel, A., Ben-Ezra, D., Shpigel, M., Addadi, L., Weiner, S., 2016. Calcium transport into the cells of the sea urchin larva in relation to spicule formation. Proc. Natl. Acad. Sci. U. S. A. http://dx.doi.org/10.1073/pnas.1612017113.

Whitehead, A., 2014. Evolutionary genomics of environmental pollution. Adv. Exp. Med. Biol. 781, 321–337. http://dx.doi.org/10.1007/978-94-007-7347-9_16.

Williams, S.E., Shoo, L.P., Isaac, J.L., Hoffmann, A.A., Langham, G., 2008. Towards an integrated framework for assessing the vulnerability of species to climate change. PLoS Biol. 6 (12), 325. http://dx.doi.org/10.1371/journal.pbio.0060325.

Wilt, F.H., 2005. Developmental biology meets materials science: morphogenesis of biomineralized structures. Dev. Biol. 280, 15–25. http://dx.doi.org/10.1016/j.ydbio.2005.01.019.

Yang, X.C., Sachs, F., 1989. Block of stretch-activated ion channels in Xenopus oocytes by gadolinium and calcium ions. Science 243, 1068–1071.

Zhu, Y., Hoshino, M., Yamada, H., Itoh, A., Haraguchi, H., 2004. Gadolinium anomaly in the distributions of rare earth elements observed for coastal seawater and river waters around Nagoya. City Bull. Chem. Soc. Jpn. 77, 1835–1842. http://dx.doi.org/10.1246/bcsj.77.1835.

Zito, F., Koop, D., Byrne, M., Matranga, V., 2015. Carbonic anhydrase inhibition blocks skeletogenesis and echinochrome production in *Paracentrotus lividus* and *Heliocidaris tuberculata* embryos and larvae. Dev. Growth Differ. 57, 507–514. http://dx.doi.org/10.1111/dgd.12229.